BIO DESIGN

pISSN 2288-6982 | eISSN 2288-7105

MINI REVIEW P 13-19

3D Electron Microscopy
: A Versatile and Unique Tool for Structural Biology

Jae-Kyung Hyun* and Hyun Suk Jung*
Division of Electron Microscopic Research, Korea Basic Science Institute, 169-148 Gwanhak-ro, Daejeon 305-308, Korea.
*Correspondence: J.K.Hyun; hjk002@kbsi.re.kr, H.S.Jung; hyunsukjung@kbsi.re.kr

Transmission electron microscopy (TEM) is a versatile and powerful technique that enables direct visualization of biological samples of sizes ranging from whole cell to near-atomic resolution details of a protein molecule. Thanks to numerous technical breakthroughs and monumental discoveries, 3D electron microscopy (3DEM) has become an indispensable tool in the field of structural biology. In particular, development of cryo-electron microscopy and computational image processing played pivotal role for the determination of 3D structures of complex biological systems at sub-molecular resolution. Analysis of crystalline object, single particle analysis and electron tomography are among the most widely used 3DEM approaches, and each technique has unique advantages depending on the nature of the biological specimen. While 3DEM analysis is now routinely performed using various resources that are publically available, the technique is constantly evolving in order to understand biological insights that were once considered impossible.

INTRODUCTION

Since its invention in 1930s by Ernst Ruska, transmission electron microscope (TEM) has become an essential imaging tool for researchers in various disciplines. In particular, TEM uses high voltage electrons as an illumination source to generate projection images that provide sufficient structural information of biological samples of size ranging from cell to protein molecules. Due to its versatility, TEM allows to fill in the gap between biological imaging at cellular level, often provided by light microscopy, and structure determination at atomic level that are usually studied using x-ray crystallography and nuclear magnetic resonance (NMR) spectroscopy. The uniqueness of TEM-mediated biological imaging largely owes to “direct” visualization of nano-scale structures that does not rely on spectroscopic analysis and/or modification of native biological states derived from undesirable crystal packing. This is particularly true when the specimen is preserved in frozen-hydrated state through the cryogenic technique, so called cryo-electron microscopy (cryo-EM).

Cryo-EM utilizes rapid freezing of wet biological specimen to liquid nitrogen temperature, which causes water to become amorphous, glass-like state without formation of crystalline ice, hence perfectly entrapping the native structure of the specimen that is suitable for TEM imaging (Dubochet et al., 1988; Taylor and Glaeser, 1974). Furthermore, imaging of frozen-hydrated specimen does not suffer from sample deformation and dehydration of conventional staining methods that delimits achievable resolution to about 2 nm (Bremer et al., 1992; Ohi et al., 2004). However, electron beam-induced radiation damage (Egerton et al., 2004; Glaeser, 1971) necessitates limited electron dose applied to biological materials that has intrinsically weak electron scattering, hence producing low contrast images. In order to compensate this, the use computational image processing and subsequent extraction of high resolution structural information has become mandatory.

The image processing is based on averaging projection images taken from micrographs that contain identical particle images that ultimately results in reduced random noise while enhancing the signal from the particles (Markham et al., 1963). Image processing was initially attempted for large assemblies with repeating protein motifs such as protein 2D crystals, helical assemblies and icosahedral viruses (Crowther et al., 1970; De Rosier and Klug, 1968; Henderson and Unwin, 1975). Later, the method was successfully applied to smaller protein complexes with little or no symmetry due to improved alignment and classification algorithms (Frank et al., 1981). Most importantly, image processing made possible to reconstruct 3D volume out of 2D projection images by either merging the images of manually tilted specimen or by estimating relative orientation of the projection images of particles. On the other hand, development of electron tomography extended the range of 3D analysis toward cellular level although high resolution structure determination by image averaging is precluded (Frank, 1995; Koster et al., 1997).

Depending on the nature of biological specimen, 3D electron microscopy (3DEM) approach can be largely divided into three categories; analysis of ordered protein assemblies, single

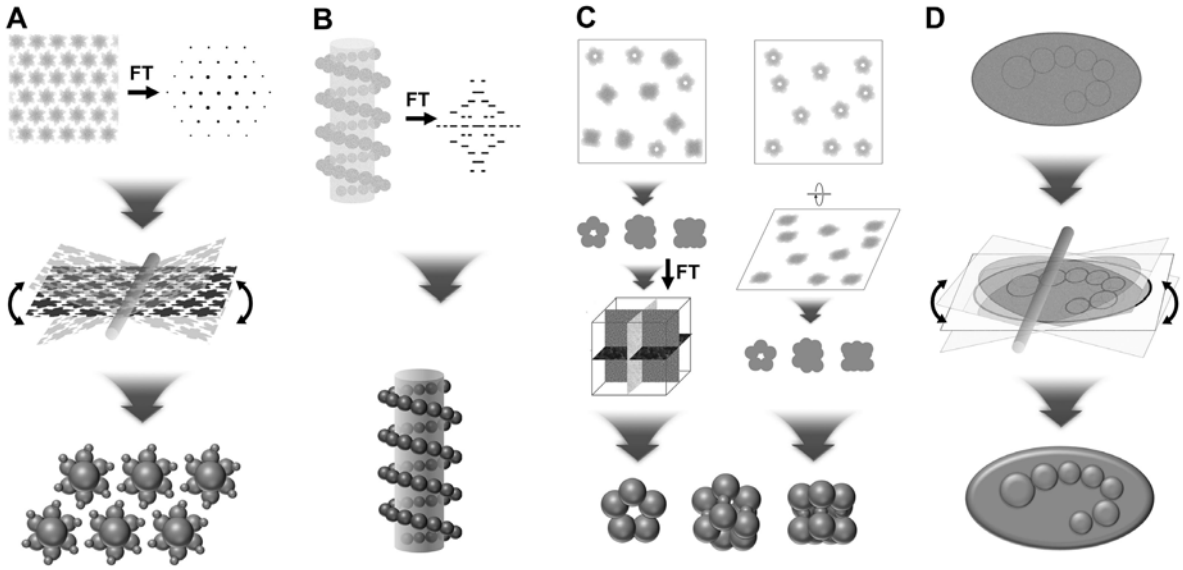

FIGURE 1 | Schematic illustration of various 3DEM approaches. (A) Electron crystallography of planar 2D arrays, (B) helical 3D reconstruction, (C) single particle analysis of macromolecular complexes and (D) electron tomography of large, irregular structures. All methods aim to generate 3D model from noisy projection images recorded from TEM.

particle analysis approach for macromolecular complexes, and electron tomography for large sub-cellular components. While sample preparation methods, image processing techniques and milestones of 3DEM are well-documented elsewhere (Chang et al., 2012; Frank, 2009; Grassucci et al., 2008; Hurbain and Sachse, 2011; Orlova and Saibil, 2011; Ubarretxena-Belandia and Stokes, 2010; Zhou, 2011) in this review, brief introductions to analytical techniques and some of the recent breakthroughs are described, and also current efforts that attempts to evolve 3DEM into the next level are discussed.

3DEM OF ORDERED ASSEMBLIES

Electron crystallography of planar array of proteins provides ideal scenario for high resolution structural analysis because a single micrograph contains copies of identical protein in a regular repeats and such ordered array can be processed using Fourier filtration (Figure 1A) (Amos et al., 1982; Jap et al., 1992). The technique utilizes Fourier transform of the micrograph for extraction of structure factors that are represented as diffraction spots while background noise is eliminated by masking those spots (Crowther et al., 1996). Unlike x-ray crystallography that utilizes diffraction data that only contains amplitude information and the phase is determined using other means such as molecular replacement and isomorphous replacement (Taylor, 2003), Fourier transform of the electron micrograph retains both phase (shape) and amplitude (intensity) of the structure. However, it is to be noted that reduced data resolution derived from the imperfect recording of the specimen often necessitates acquisition of electron diffraction directly from the microscope, and hence molecular replacement or phase extension from low resolution phases of recorded images are required (Gonen et al., 2005; Wisedchaisri and Gonen, 2011). One of the critical steps in structural analysis using electron crystallography is computational "unbending" of distortions within the crystal (Crowther et al., 1996; Jeong et al., 2013). In most cases, protein crystals are not perfectly ordered, and therefore a small region with the best crystalline order within the micrograph serves as a reference for the cross-correlation-based correction for image distortion. The reference region may be selected from the best diffraction quality as examined from optical diffraction of negative films or from local Fourier transforms from digitized micrographs. Consequently, successful unbending results in the extraction of high-resolution information high fidelity.

Electron crystallography of protein was first applied to naturally occurring 2D crystal, purple membrane from *Halobacterium halobium*, and had proven its potential for high resolution structure determination (Henderson and Unwin, 1975). Subsequently, numerous protein structures have been studied to molecular levels (Auer et al., 1998; Bostina et al., 2005; Unger et al., 1999) and also at near-atomic resolutions (Gonen et al., 2005; Kimura et al., 1997; Tani et al., 2009). In particular, electron crystallography found niche in the field of structural biology for its unique application in the analysis of membrane proteins (Bill et al., 2011; Wisedchaisri et al., 2011). Membrane proteins can be reconstituted into lipid bilayer in their native environment and successful crystallization may lead to high resolution structure determination (Abeyrathne et al., 2010). However, major bottleneck of this technique is the need for protein crystallization,

which involves intensive manual screening of crystallization conditions with relatively low success rate. Inefficiency of this technique and emergence of single particle analysis (SPA) as an excellent alternative for 3DEM of soluble protein complexes hampers routine use of electron crystallography. Inevitably, recent technical developments heavily focus on high-throughput crystallization screening by the use of automatic systems (Ubarretxena-Belandia and Stokes, 2010). For instance, lipid-to-protein ratio, type of detergent and rate of detergent removal can be controlled by robotic system in a manner that is similar to crystallization robots used by x-ray crystallographers (Iacovache et al., 2010; Vink et al., 2007). Although the formation of 2D crystals can only be confirmed by loading the specimen into TEM, which is still labor-intensive, automated sample loading device has been developed (Cheng et al., 2007; Kim et al., 2010a). Additional developments include user-friendly software package, such as 2dx, that allows automized image processing for novice users (Gipson et al., 2007a; Gipson et al., 2007b). Moreover, software tools for the automated analysis of electron diffraction for advanced, high resolution analysis have been developed (Philippsen et al., 2003; Schenk et al., 2013). Also, typical "missing cone effect" that is derived from limited tilt angle of the specimen relative to electron beam, as a result producing anisotropic 3D resolution, is partially resolved by recent application of projective constraint optimization in image processing routine (Gipson et al., 2011).

In terms of using a regular repeats of molecular densities, elongated protein assemblies that exhibit uniform helical repeats can be regarded as rolled-up 2D crystals, and suitable for Fourier filtration as in the case of electron crystallography (Diaz et al., 2010) (Figure 1B). It is to be noted that helical assemblies not only provide thousands of repeating motif in a micrograph, but also offers visualization of multiple orientation of asymmetric units, and hence tilting of the specimen becomes unnecessary. Naturally occurring examples include helical viruses (De Rosier and Klug, 1968; Ge and Zhou, 2011) and cytoskeletal components such as actin and microtubules (Moore et al., 1970; Reisler and Egelman, 2007) as well as bacterial flagella (O'Brien and Bennett, 1972; Yonekura et al., 2003). In addition, protein-enriched cellular membranes may form tubular crystals as in the case of nicotinic acetylcholine receptor, a neurotransmitter-gated ion channel (Unwin, 1995, 2005). It is also possible to induce the proteins to form helically ordered assemblies by providing tubular lipid platform that has specific affinity to the target protein (Wilson-Kubalek et al., 1998). In terms of image processing, traditional Fourier-Bessel reconstruction method (Diaz et al., 2010) and more recent iterative helical real-space iteration reconstruction are widely used (Egelman, 2007).

SINGLE PARTICLE ANALYSIS

As the name indicates, single particle analysis (SPA) is employed to obtain structural information from micrographs that contain copies of identical protein complex without the need for the formation of ordered arrays such as 2D crystals (Thuman-Commike, 2001) (Figure 1C). In contrast to electron crystallography, from which the structural information can be selectively extracted from discrete diffraction spots, SPA requires micrographs containing homogeneous protein complexes in order to extract enhanced signal and reduce random noise present in raw images. While the essence of 2D analysis is grouping similar particle images and bringing them to a register in order to generate "class averages", it is critical to estimate relative orientation of a particle from projection images for building a reliable 3D reconstruction. Class averaging is achieved by centering, rotation and translation of individual images in the dataset with respect to multiple reference images, from which the previous iteration serve as new references for the subsequent round of iteration using statistical analysis (Frank, 1981; Ludtke et al., 1999; van Heel and Frank, 1981). In order to eliminate model bias, references are initially built from random averaging of subsets, and are iteratively refined. Whereas conventional method assigns a particle image to a reference with the highest cross correlation, a more recently introduced maximum likelihood algorithm employs probability-weighted averages over all possible alignments (Scheres, 2012; Scheres et al., 2005). Once suitable class averages are generated, relative orientation of the particles must be estimated in order to merge the projection images into a 3D volume (Kim et al., 2010b). When the particles are adsorbed onto the specimen grid with a preferential orientation, available view of the particle becomes limited. In such a case, "random conical tilt" method may be employed where the images of tilted and untilted specimen are recorded for a given field of view (Radermacher et al., 1987). As a result, the variation of particle orientation is improved, and since the tilt angles are known, orientation of tilted particles relative to untilted particles can be determined. Alternatively, orientation search for randomly oriented particles can be carried out using "common lines" approach which is based on central section theorem. The theorem states that the Fourier transform of any two 2D projections of the same 3D object intersect at a common 1D projection line. Applied to SPA, angles between the common lines from the images of particles in various orientations are used to determine relative orientation of the particles (van Heel, 1987). Particles images are then matched to 2D projections of coarse *ab initio* 3D model in order to refine the orientation iteratively (van Heel et al., 2000).

In order to achieve high-resolution 3D structure determination using SPA, tens to hundreds of thousands particle images are required because accumulation of similar, low-contrast particle images results in enhanced high-resolution features. For this reason, collection of data and image processing are often time-consuming and labor-intensive, especially for particles that lack symmetry since each orientation can be represented by a single projection view. This has been greatly improved by the use of field emission gun (FEG) that generates more coherent electron beam than conventionally used LaB_6 or tungsten (Zhou

and Chiu, 1993). Also, image recoding aided by direct detection device (DDD) with superior detective quantum efficiency (DQE) increased the content of high-resolution information in individual micrograph in comparison to photographic film and charge-coupled device (CCD) camera (Bammes et al., 2012; Li et al., 2013). In addition, recently developed DDDs are capable of recording images with high frame rate, allowing for capturing and compensating for beam-induced particle movement of vitrified specimen, which in turn facilitates high-resolution structure determination (Bai et al., 2013). In both cases, resolution-dependent attenuation of structural information, termed envelope function (Sorzano et al., 2007), is improved and therefore required number of images is significantly reduced (Bai et al., 2013). Rigorous manual data acquisition is being replaced by recently introduced automization tools that allows for the collection of large dataset (Lei and Frank, 2005; Suloway et al., 2005), and in addition, real-time image processing that can monitor 3D structure is being developed (Cardone et al., 2013).

ELECTRON TOMOGRAPHY

Unlike other 3DEM methods that rely on averaging of similar particle images, electron tomography (ET) enables 3D structure determination of large cellular and sub-cellular components that lacks morphological homogeneity (Hoenger and Bouchet-Marquis, 2011). ET involves tilting of the specimen inside TEM and collection of images at varying orientations, from which a 3D reconstruction is computationally generated by alignment and merging of image stack (Lucic et al., 2013) (Figure 1D). The technique gained additional momentum by application of cryo-EM to whole cells and tissues, which allows for 3D visualization of cellular ultrastructure without artifacts derived from chemical fixation and staining (Heuser, 2002). For cryo-electron tomography (cryo-ET), the sample is either cryogenically fixed by high-pressure freezing followed by slow dehydration and resin-embedment (Hurbain and Sachse, 2011; Studer et al., 2008), or by using cryo-ultramicrotome to section frozen sample directly (Al-Amoudi et al., 2004). Whereas sectioning of the sample is inevitable due to limited penetration of electron beam, typically up to ~500 nm for TEM operating at 200 – 300 kV (Koster et al., 1997), thinner samples such as bacteria or peripheral regions of eukaryotic cells can be readily used for tomographic analysis through vitrification alone (Milne et al., 2013). Although technically demanding for frozen-hydrated specimen, use of even higher acceleration voltage, as in the case of high-voltage electron microscope operating at over 1000 kV, promises tomographic analysis of thicker samples due to enhanced electron beam penetration (Glauert, 1974; Tanaka et al., 2013). Because no averaging is used for the enhancement of high-resolution information, achievable resolution is far inferior to other techniques, typically at 4 - 5 nm, with the exception of sub-tomogram averaging from which regular structures from electron tomogram are averaged (Nickell et al., 2007; Schmid, 2011). Moreover, limited tilt angle of the specimen in the microscope causes “missing wedge”, which results in incomprehensive 3D information of the reconstruction and undesirable distortions. While specially designed specimen holders may be used to maximize possible tilt angle, tilting the specimen around two tilt axes that are perpendicular improves completeness of the reconstruction with isotropic resolution (Mastronarde, 1997). Despite certain disadvantages associated with the structural analysis using ET, numerous biological systems are being studied with previously unknown insights with moderate details. Examples include cytoskeletal network inside the cell (Li et al., 2012; Pilhofer et al., 2010), entry and propagation of viruses in host cells (Briggs et al., 2009; Chlanda et al., 2011) and motor system involved in bacterial mobility (Raddi et al., 2012; Ruan et al., 2012). In fact, cryo-ET is now regarded as a powerful tool that can fill in the gap between light microscopy and electron microscopy, providing 3D visualization of biological systems in their native environment.

FUTURE OF TEM-MEDIATED BIOLOGICAL IMAGING

TEM by itself offers excellent tool for structural biology at molecular level, with increasing number of near-atomic resolution 3D structure determination being published (Figure 2). However, true versatility of 3DEM comes from its compatibility with other approaches. Atomic structures of individual proteins or subunits, usually obtained by x-ray crystallography and NMR spectroscopy, are now routinely docked into moderate resolution 3DEM density map of a whole complex in order to define inter-molecular interactions that govern biological functions (Rossmann et al., 2005). More recently, combinatorial efforts have broadened over various 3DEM techniques (Robinson et al., 2007). For example, structure of authentic HIV-1 capsid have been elucidated from *in vivo* imaging by cryo-ET, 3D structure determination of symmetric components using electron crystallography and SPA of *in vitro* assemblies, and atomic structure determination of individual subunits as solved by x-ray crystallography and NMR (Yeager, 2011). More systematic hybrid approaches are being applied in practice using template matching, where low-resolution electron tomogram serves as a template into which high resolution structures are fitted, hence providing static view of each protein complexes in action (Beck et al., 2011; Kuhner et al., 2009). Moreover, in order to compensate static TEM imaging of biological specimen, correlative light-electron microscopy has been recently developed (van Driel et al., 2009). While dynamic cellular process can be monitored by light microscopy with specific events are guided by fluorescent signal, the specimen is rapidly immobilized via vitrification and the target area mapped on EM grid can be subjected to cryo-ET, providing correlative *in situ* analysis (Hanein and Volkmann, 2011).

Technical hurdles preclude certain TEM techniques to be applied to biological specimen. Such applications include electron energy loss spectroscopy (EELS) and energy dispersive x-ray spectroscopy (EDS), which are strictly limited to inorganic

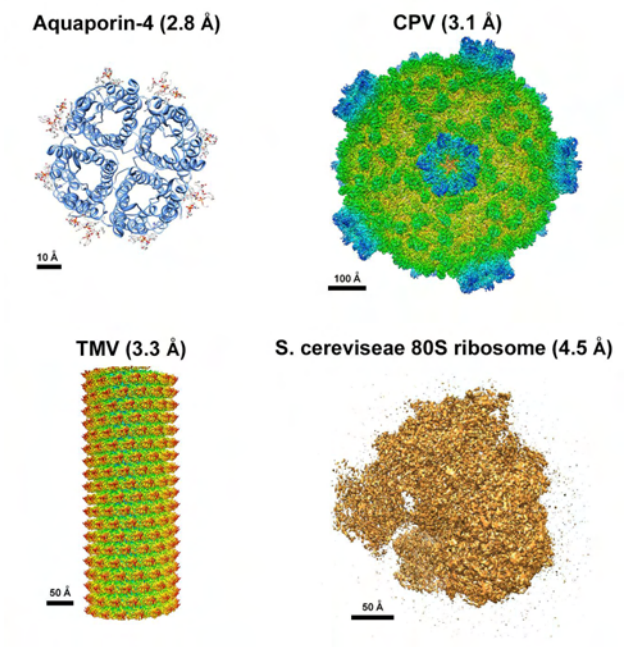

FIGURE 2 | Examples of near-atomic resolution 3DEM structures. Representative near-atomic models: aquaporin (electron crystallography, PDB ID 2ZZ9), cytoplasmic polyhedrosis virus (SPA, EMDB ID 5256), tobacco mosaic virus (helical reconstruction, EMDB ID 5185) and S. cereviseae 80S ribosome (SPA, EMDB ID 2275). UCSF Chimera (Pettersen et al., 2004) was used for visualization of PDB (http://www.rcsb.org) and EMDB (http://www.emdatabank.org) structures.

materials at current technology due to radiation damage and undetectable concentration of cellular chemicals (Egerton et al., 2004). However, once technical barriers are overcome through the technical development of highly sensitive instruments, real-time analysis of localization and movement of certain chemicals in context of biological system may be possible. Also, it has recently become evident that the use of graphene sheet can entrap liquid in an isolated environment unaffected by vacuum of a TEM as demonstrated by material scientists (Yuk et al., 2012). Analysis of biological sample in similar manner is much more complicated due to radiation damage and complexity of specimen, but attempts are being made to avoid such problems (de Jonge and Ross, 2011). In addition, application of ultrafast laser electron microscopy (UEM) may allow true time-resolved analysis of dynamic changes that take place in biological systems (Zewail, 2010). With these unconventional hybrid approaches, 3DEM have yet another potential to evolve into an imaging tool that can realize what was once regarded impossible.

ABBREVIATIONS

2D	Two dimensional
3D	Three dimensional
3DEM	Three dimensional electron microscopy
CCD	Charge-coupled device
Cryo-EM	Cryo-electron microscopy
Cryo-ET	Cryo-electron tomography
DDD	Direct detection device
DQE	Detective quantum efficiency
EDS	Energy dispersive x-ray spectroscopy
EELS	Electron energy loss spectroscopy
ET	Electron tomography
FEG	Field emission gun
HIV	Human immunodeficiency virus
NMR	Nuclear magnetic resonance
SPA	Single particle analysis
TEM	Transmission electron microscopy
UEM	Ultrafast laser electron microscopy

ACKNOWLEDGEMEANTS

This work was supported by Converging Research Center Program through the National Research Foundation of Korea funded by the Ministry of Education, Science and Technology (2012K001403) and by Korea Basic Science Institute grant (T33518).

Original Submission: October 1, 2013
Revised Version Received: November 14, 2013
Accepted: November 19, 2013

REFERENCES

Abeyrathne, P.D., Chami, M., Pantelic, R.S., Goldie, K.N., and Stahlberg, H. (2010). Preparation of 2D crystals of membrane proteins for high-resolution electron crystallography data collection. *Methods Enzymol* **481**, 25-43.

Al-Amoudi, A., Chang, J.J., Leforestier, A., McDowall, A., Salamin, L.M., Norlen, L.P., Richter, K., Blanc, N.S., Studer, D., and Dubochet, J. (2004). Cryo-electron microscopy of vitreous sections. *EMBO J* **23**, 3583-3588.

Amos, L.A., Henderson, R., and Unwin, P.N. (1982). Three-dimensional structure determination by electron microscopy of two-dimensional crystals. *Prog Biophys Mol Biol* **39**, 183-231.

Auer, M., Scarborough, G.A., and Kuhlbrandt, W. (1998). Three-dimensional map of the plasma membrane H+-ATPase in the open conformation. *Nature* **392**, 840-843.

Bai, X.C., Fernandez, I.S., McMullan, G., and Scheres, S.H. (2013). Ribosome structures to near-atomic resolution from thirty thousand cryo-EM particles. *Elife* **2**, e00461.

Bammes, B.E., Rochat, R.H., Jakana, J., Chen, D.H., and Chiu, W. (2012). Direct electron detection yields cryo-EM reconstructions at resolutions beyond 3/4 Nyquist frequency. *J Struct Biol* **177**, 589-601.

Beck, M., Topf, M., Frazier, Z., Tjong, H., Xu, M., Zhang, S., and Alber, F. (2011). Exploring the spatial and temporal organization of a cell's proteome. *J Struct Biol* **173**, 483-496.

Bill, R.M., Henderson, P.J., Iwata, S., Kunji, E.R., Michel, H., Neutze, R., Newstead, S., Poolman, B., Tate, C.G., and Vogel, H. (2011). Overcoming

barriers to membrane protein structure determination. *Nat Biotechnol* **29**, 335-340.

Bostina, M., Mohsin, B., Kuhlbrandt, W., and Collinson, I. (2005). Atomic model of the E. coli membrane-bound protein translocation complex SecYEG. *J Mol Biol* **352**, 1035-1043.

Bremer, A., Henn, C., Engel, A., Baumeister, W., and Aebi, U. (1992). Has negative staining still a place in biomacromolecular electron microscopy? *Ultramicroscopy* **46**, 85-111.

Briggs, J.A., Riches, J.D., Glass, B., Bartonova, V., Zanetti, G., and Krausslich, H.G. (2009). Structure and assembly of immature HIV. *Proc Natl Acad Sci U S A* **106**, 11090-11095.

Cardone, G., Yan, X., Sinkovits, R.S., Tang, J., and Baker, T.S. (2013). Three-dimensional reconstruction of icosahedral particles from single micrographs in real time at the microscope. *J Struct Biol* **183**, 329-341.

Chang, J., Liu, X., Rochat, R.H., Baker, M.L., and Chiu, W. (2012). Reconstructing virus structures from nanometer to near-atomic resolutions with cryo-electron microscopy and tomography. *Adv Exp Med Biol* **726**, 49-90.

Cheng, A., Leung, A., Fellmann, D., Quispe, J., Suloway, C., Pulokas, J., Abeyrathne, P.D., Lam, J.S., Carragher, B., and Potter, C.S. (2007). Towards automated screening of two-dimensional crystals. *J Struct Biol* **160**, 324-331.

Chlanda, P., Carbajal, M.A., Kolovou, A., Hamasaki, M., Cyrklaff, M., Griffiths, G., and Krijnse-Locker, J. (2011). Vaccinia virus lacking A17 induces complex membrane structures composed of open membrane sheets. *Arch Virol* **156**, 1647-1653.

Crowther, R.A., Amos, L.A., Finch, J.T., De Rosier, D.J., and Klug, A. (1970). Three dimensional reconstructions of spherical viruses by fourier synthesis from electron micrographs. *Nature* **226**, 421-425.

Crowther, R.A., Henderson, R., and Smith, J.M. (1996). MRC image processing programs. *J Struct Biol* **116**, 9-16.

de Jonge, N., and Ross, F.M. (2011). Electron microscopy of specimens in liquid. *Nat Nanotechnol* **6**, 695-704.

De Rosier, D.J., and Klug, A. (1968). Reconstruction of three dimensional structures from electron micrographs. *Nature* **217**, 130134.

Diaz, R., Rice, W.J., and Stokes, D.L. (2010). Fourier-Bessel reconstruction of helical assemblies. *Methods Enzymol* **482**, 131-165.

Dubochet, J., Adrian, M., Chang, J.J., Homo, J.C., Lepault, J., McDowall, A.W., and Schultz, P. (1988). Cryo-electron microscopy of vitrified specimens. *Q Rev Biophys* **21**, 129-228.

Egelman, E.H. (2007). The iterative helical real space reconstruction method: surmounting the problems posed by real polymers. *J Struct Biol* **157**, 83-94.

Egerton, R.F., Li, P., and Malac, M. (2004). Radiation damage in the TEM and SEM. *Micron* **35**, 399-409.

Frank, J. (1981). Three-dimensional reconstruction of single molecules. *Methods Cell Biol* **22**, 325-344.

Frank, J. (1995). Approaches to large-scale structures. *Curr Opin Struct Biol* **5**, 194-201.

Frank, J. (2009). Single-particle reconstruction of biological macromolecules in electron microscopy--30 years. *QQ Rev Biophys* **42**, 139-158.

Frank, J., Verschoor, A., and Boublik, M. (1981). Computer averaging of electron micrographs of 40S ribosomal subunits. *Science* **214**, 1353-1355.

Ge, P., and Zhou, Z.H. (2011). Hydrogen-bonding networks and RNA bases revealed by cryo electron microscopy suggest a triggering mechanism for calcium switches. *Proc Natl Acad Sci U S A* **108**, 9637-9642.

Gipson, B., Zeng, X., and Stahlberg, H. (2007a). 2dx_merge: data management and merging for 2D crystal images. *J Struct Biol* **160**, 375-384.

Gipson, B., Zeng, X., Zhang, Z.Y., and Stahlberg, H. (2007b). 2dx--user-friendly image processing for 2D crystals. *J Struct Biol* **157**, 64-72.

Gipson, B.R., Masiel, D.J., Browning, N.D., Spence, J., Mitsuoka, K., and Stahlberg, H. (2011). Automatic recovery of missing amplitudes and phases in tilt-limited electron crystallography of two-dimensional crystals. *Phys Rev E Stat Nonlin Soft Matter Phys* **84**, 011916.

Glaeser, R.M. (1971). Limitations to significant information in biological electron microscopy as a result of radiation damage. *J Ultrastruct Res* **36**, 466-482.

Glauert, A.M. (1974). The high voltage electron microscope in biology. *J Cell Biol* **63**, 717-748.

Gonen, T., Cheng, Y., Sliz, P., Hiroaki, Y., Fujiyoshi, Y., Harrison, S.C., and Walz, T. (2005). Lipid-protein interactions in double-layered two-dimensional AQP0 crystals. *Nature* **438**, 633-638.

Grassucci, R.A., Taylor, D., and Frank, J. (2008). Visualization of macromolecular complexes using cryo-electron microscopy with FEI Tecnai transmission electron microscopes. *Nat Protoc* **3**, 330-339.

Hanein, D., and Volkmann, N. (2011). Correlative light-electron microscopy. *Adv Protein Chem Struct Biol* **82**, 91-99.

Henderson, R., and Unwin, P.N. (1975). Three-dimensional model of purple membrane obtained by electron microscopy. *Nature* **257**, 28-32.

Heuser, J. (2002). Whatever happened to the 'microtrabecular concept'? *Biol Cell* **94**, 561-596.

Hoenger, A., and Bouchet-Marquis, C. (2011). Cellular tomography. *Adv Protein Chem Struct Biol* **82**, 67-90.

Hurbain, I., and Sachse, M. (2011). The future is cold: cryo-preparation methods for transmission electron microscopy of cells. *Biol Cell* **103**, 405-420.

Iacovache, I., Biasini, M., Kowal, J., Kukulski, W., Chami, M., van der Goot, F.G., Engel, A., and Remigy, H.W. (2010). The 2DX robot: a membrane protein 2D crystallization Swiss Army knife. *J Struct Biol* **169**, 370-378.

Jap, B.K., Zulauf, M., Scheybani, T., Hefti, A., Baumeister, W., Aebi, U., and Engel, A. (1992). 2D crystallization: from art to science. *Ultramicroscopy* **46**, 45-84.

Jeong, H.S., Park, H.N., Kim, J.G., and Hyun, J.K. (2013). Critical importance of the correction of contrast transfer function for transmission electron microscopy-mediated structural biology. *Journal of Analytical Science and Technology* **4**, 14-19.

Kim, C., Vink, M., Hu, M., Love, J., Stokes, D.L., and Ubarretxena-Belandia, I. (2010a). An automated pipeline to screen membrane protein 2D crystallization. *J Struct Funct Genomics* **11**, 155-166.

Kim, S.J., Jeong, J.M., Kim, C.H., Park, S.O., Ryu, K.Y., Kwon, H.S., and Jung, H.S. (2010b). The use of artificial structure as an initial reference model for projection-matching three dimensional reconstructurion: vizualization of macromolecular structure using cryo-electron microscopy. *Journal of Analytical Science and Technology* **1**, 159-164.

Kimura, Y., Vassylyev, D.G., Miyazawa, A., Kidera, A., Matsushima, M., Mitsuoka, K., Murata, K., Hirai, T., and Fujiyoshi, Y. (1997). Surface of bacteriorhodopsin revealed by high-resolution electron crystallography. *Nature* **389**, 206-211.

Koster, A.J., Grimm, R., Typke, D., Hegerl, R., Stoschek, A., Walz, J., and Baumeister, W. (1997). Perspectives of molecular and cellular electron tomography. *J Struct Biol* **120**, 276-308.

Kuhner, S., van Noort, V., Betts, M.J., Leo-Macias, A., Batisse, C., Rode, M., Yamada, T., Maier, T., Bader, S., Beltran-Alvarez, P., et al. (2009). Proteome organization in a genome-reduced bacterium. *Science* **326**, 1235-1240.

Lei, J., and Frank, J. (2005). Automated acquisition of cryo-electron micrographs for single particle reconstruction on an FEI Tecnai electron microscope. *J Struct Biol* **150**, 69-80.

Li, S., Fernandez, J.J., Marshall, W.F., and Agard, D.A. (2012). Three-dimensional structure of basal body triplet revealed by electron cryo-tomography. *EMBO J* **31**, 552-562.

Li, X., Mooney, P., Zheng, S., Booth, C.R., Braunfeld, M.B., Gubbens, S., Agard, D.A., and Cheng, Y. (2013). Electron counting and beam-induced motion correction enable near-atomic-resolution single-particle cryo-EM. *Nat Methods* **10**, 584-590.

Lucic, V., Rigort, A., and Baumeister, W. (2013). Cryo-electron tomography: the challenge of doing structural biology in situ. *J Cell Biol* **202**, 407-419.

Ludtke, S.J., Baldwin, P.R., and Chiu, W. (1999). EMAN: semiautomated software for high-resolution single-particle reconstructions. *J Struct Biol* **128**, 82-97.

Markham, R., Frey, S., and Hills, G.J. (1963). Methods for the enhancement of image detail and accentuation of structure in electron microscopy. *Virology* **20**, 88-102.

Mastronarde, D.N. (1997). Dual-axis tomography: an approach with alignment methods that preserve resolution. *J Struct Biol* **120**, 343-352.

Milne, J.L., Borgnia, M.J., Bartesaghi, A., Tran, E.E., Earl, L.A., Schauder, D.M., Lengyel, J., Pierson, J., Patwardhan, A., and Subramaniam, S. (2013). Cryo-electron microscopy--a primer for the non-microscopist. *FEBS J* **280**, 28-45.

Moore, P.B., Huxley, H.E., and DeRosier, D.J. (1970). Three-dimensional reconstruction of F-actin, thin filaments and decorated thin filaments. *J Mol Biol* **50**, 279-295.

Nickell, S., Mihalache, O., Beck, F., Hegerl, R., Korinek, A., and Baumeister, W. (2007). Structural analysis of the 26S proteasome by cryoelectron tomography. *Biochem Biophys Res Commun* **353**, 115-120.

O'Brien, E.J., and Bennett, P.M. (1972). Structure of straight flagella from a mutant Salmonella. *J Mol Biol* **70**, 133-152.

Ohi, M., Li, Y., Cheng, Y., and Walz, T. (2004). Negative Staining and Image Classification - Powerful Tools in Modern Electron Microscopy. *Biol Proced Online* **6**, 23-34.

Orlova, E.V., and Saibil, H.R. (2011). Structural analysis of macromolecular assemblies by electron microscopy. *Chem Rev* **111**, 7710-7748.

Pettersen, E.F., Goddard, T.D., Huang, C.C., Couch, G.S., Greenblatt, D.M., Meng, E.C., and Ferrin, T.E. (2004). UCSF Chimera--a visualization system for exploratory research and analysis. *J Comput Chem* **25**, 1605-1612.

Philippsen, A., Schenk, A.D., Stahlberg, H., and Engel, A. (2003). Iplt--image processing library and toolkit for the electron microscopy community. *J Struct Biol* **144**, 4-12.

Pilhofer, M., Ladinsky, M.S., McDowall, A.W., and Jensen, G.J. (2010). Bacterial TEM: new insights from cryo-microscopy. *Methods Cell Biol* **96**, 21-45.

Raddi, G., Morado, D.R., Yan, J., Haake, D.A., Yang, X.F., and Liu, J. (2012). Three-dimensional structures of pathogenic and saprophytic Leptospira species revealed by cryo-electron tomography. *J Bacteriol* **194**, 1299-1306.

Radermacher, M., Wagenknecht, T., Verschoor, A., and Frank, J. (1987). Three-dimensional reconstruction from a single-exposure, random conical tilt series applied to the 50S ribosomal subunit of Escherichia coli. *J Microsc* **146**, 113-136.

Reisler, E., and Egelman, E.H. (2007). Actin structure and function: what we still do not understand. *J Biol Chem* **282**, 36133-36137.

Robinson, C.V., Sali, A., and Baumeister, W. (2007). The molecular sociology of the cell. *Nature* **450**, 973-982.

Rossmann, M.G., Morais, M.C., Leiman, P.G., and Zhang, W. (2005). Combining X-ray crystallography and electron microscopy. *Structure* **13**, 355-362.

Ruan, J., Kato, T., Santini, C.L., Miyata, T., Kawamoto, A., Zhang, W.J., Bernadac, A., Wu, L.F., and Namba, K. (2012). Architecture of a flagellar apparatus in the fast-swimming magnetotactic bacterium MO-1. *Proc Natl Acad Sci U S A* **109**, 20643-20648.

Schenk, A.D., Philippsen, A., Engel, A., and Walz, T. (2013). A pipeline for comprehensive and automated processing of electron diffraction data in IPLT. *J Struct Biol* **182**, 173-185.

Scheres, S.H. (2012). RELION: implementation of a Bayesian approach to cryo-EM structure determination. *J Struct Biol* **180**, 519-530.

Scheres, S.H., Valle, M., Nunez, R., Sorzano, C.O., Marabini, R., Herman, G.T., and Carazo, J.M. (2005). Maximum-likelihood multi-reference refinement for electron microscopy images. *J Mol Biol* **348**, 139-149.

Schmid, M.F. (2011). Single-particle electron cryotomography (cryoET). *Adv Protein Chem Struct Biol* **82**, 37-65.

Sorzano, C.O., Jonic, S., Nunez-Ramirez, R., Boisset, N., and Carazo, J.M. (2007). Fast, robust, and accurate determination of transmission electron microscopy contrast transfer function. *J Struct Biol* **160**, 249-262.

Studer, D., Humbel, B.M., and Chiquet, M. (2008). Electron microscopy of high pressure frozen samples: bridging the gap between cellular ultrastructure and atomic resolution. *Histochem Cell Biol* **130**, 877-889.

Suloway, C., Pulokas, J., Fellmann, D., Cheng, A., Guerra, F., Quispe, J., Stagg, S., Potter, C.S., and Carragher, B. (2005). Automated molecular microscopy: the new Leginon system. *J Struct Biol* **151**, 41-60.

Tanaka, N., Usukura, J., Kusunoki, M., Saito, Y., Sasaki, K., Tanji, T., Muto, S., and Arai, S. (2013). Development of an environmental high-voltage electron microscope for reaction science. *Microscopy (Oxf)* **62**, 205-215.

Tani, K., Mitsuma, T., Hiroaki, Y., Kamegawa, A., Nishikawa, K., Tanimura, Y., and Fujiyoshi, Y. (2009). Mechanism of aquaporin-4's fast and highly selective water conduction and proton exclusion. *J Mol Biol* **389**, 694-706.

Taylor, G. (2003). The phase problem. *Acta Crystallogr D Biol Crystallogr* **59**, 1881-1890.

Taylor, K.A., and Glaeser, R.M. (1974). Electron diffraction of frozen, hydrated protein crystals. *Science* **186**, 1036-1037.

Thuman-Commike, P.A. (2001). Single particle macromolecular structure determination via electron microscopy. *FEBS Lett* **505**, 199-205.

Ubarretxena-Belandia, I., and Stokes, D.L. (2010). Present and future of membrane protein structure determination by electron crystallography. *Adv Protein Chem Struct Biol* **81**, 33-60.

Unger, V.M., Kumar, N.M., Gilula, N.B., and Yeager, M. (1999). Three-dimensional structure of a recombinant gap junction membrane channel. *Science* **283**, 1176-1180.

Unwin, N. (1995). Acetylcholine receptor channel imaged in the open state. *Nature* **373**, 37-43.

Unwin, N. (2005). Refined structure of the nicotinic acetylcholine receptor at 4A resolution. *J Mol Biol* **346**, 967-989.

van Driel, L.F., Valentijn, J.A., Valentijn, K.M., Koning, R.I., and Koster, A.J. (2009). Tools for correlative cryo-fluorescence microscopy and cryo-electron tomography applied to whole mitochondria in human endothelial cells. *Eur J Cell Biol* **88**, 669-684.

van Heel, M. (1987). Angular reconstructuion: a posteriori assignment of projection directions for 3D reconstruction. *Ultramicroscopy* **21**, 111-124.

van Heel, M., and Frank, J. (1981). Use of multivariate statistics in analysing the images of biological macromolecules. *Ultramicroscopy* **6**, 187-194.

van Heel, M., Gowen, B., Matadeen, R., Orlova, E.V., Finn, R., Pape, T., Cohen, D., Stark, H., Schmidt, R., Schatz, M., et al. (2000). Single-particle electron cryo-microscopy: towards atomic resolution. *Q Rev Biophys* **33**, 307-369.

Vink, M., Derr, K., Love, J., Stokes, D.L., and Ubarretxena-Belandia, I. (2007). A high-throughput strategy to screen 2D crystallization trials of membrane proteins. *J Struct Biol* **160**, 295-304.

Wilson-Kubalek, E.M., Brown, R.E., Celia, H., and Milligan, R.A. (1998). Lipid nanotubes as substrates for helical crystallization of macromolecules. *Proc Natl Acad Sci U S A* **95**, 8040-8045.

Wisedchaisri, G., and Gonen, T. (2011). Fragment-based phase extension for three-dimensional structure determination of membrane proteins by electron crystallography. *Structure* **19**, 976-987.

Wisedchaisri, G., Reichow, S.L., and Gonen, T. (2011). Advances in structural and functional analysis of membrane proteins by electron crystallography. *Structure* **19**, 1381-1393.

Yeager, M. (2011). Design of in vitro symmetric complexes and analysis by hybrid methods reveal mechanisms of HIV capsid assembly. *J Mol Biol* **410**, 534-552.

Yonekura, K., Maki-Yonekura, S., and Namba, K. (2003). Complete atomic model of the bacterial flagellar filament by electron cryomicroscopy. *Nature* **424**, 643-650.

Yuk, J.M., Park, J., Ercius, P., Kim, K., Hellebusch, D.J., Crommie, M.F., Lee, J.Y., Zettl, A., and Alivisatos, A.P. (2012). High-resolution EM of colloidal nanocrystal growth using graphene liquid cells. *Science* **336**, 61-64.

Zewail, A.H. (2010). Four-dimensional electron microscopy. *Science* **328**, 187-193.

Zhou, Z.H. (2011). Atomic resolution cryo electron microscopy of macromolecular complexes. *Adv Protein Chem Struct Biol* **82**, 1-35.

Zhou, Z.H., and Chiu, W. (1993). Prospects for using an IVEM with a FEG for imaging macromolecules towards atomic resolution. *Ultramicroscopy* **49**, 407-416.